Journal of Environmental Management 232 (2019) 219–225

Contents lists available at ScienceDirect

Journal of Environmental Management

journal homepage: www.elsevier.com/locate/jenvman

Research article

Insights into the interactions between triclosan (TCS) and extracellular polymeric substance (EPS) of activated sludge

Zi-run Yan[a], Hui-shan Meng[a], Xue-yuan Yang[a], Yu-ying Zhu[a], Xiu-yan Li[a], Juan Xu[a,b,*], Guo-ping Sheng[c,**]

[a] Shanghai Key Lab for Urban Ecological Processes and Eco-Restoration, School of Ecological and Environmental Sciences, East China Normal University, Shanghai, China
[b] Institute of Eco-Chongming, East China Normal University, Shanghai, China
[c] CAS Key Laboratory of Urban Pollutant Conversion, Department of Chemistry, University of Science and Technology of China, Hefei, 230026, China

ARTICLE INFO

Keywords:
Activated sludge
Extracellular polymeric substances (EPS)
Fluorescence quenching
Interaction
Triclosan (TCS)

ABSTRACT

Triclosan (TCS) contaminant has aroused wide concerns due to the high risk of converting into toxic dioxin in aquatic environments. During the wastewater treatment process, considerable amounts of TCS are accumulated in activated sludge but the mechanisms are still unclear. Especially, roles of extracellular polymeric substances (EPS), the main components of activated sludge, in TCS removal have never been addressed. In this work, the binding properties of loosely-bound EPS (LB-EPS) and tightly-bound EPS (TB-EPS) of activated sludge to TCS are investigated by fluorescence quenching approach. The influences of aquatic conditions including solution pH, ionic strength and temperature on the interactions between EPS and TCS are explored. Possible interaction mechanisms are discussed as well as the corresponding environmental implication. Results indicate that binding processes of EPS to TCS are exothermic mainly driven by the enthalpy changes. The proteins components in EPS dominate the interactions between EPS and TCS by hydrogen bond and hydrophobic interaction. The binding strength could be improved under the condition of weak alkaline and relative high ionic strength. Generally, LB-EPS exhibit stronger binding ability to TCS than TB-EPS under neutral environment, playing more crucial roles in the binding process. This work highlights the important contributions of EPS to TCS removal, that is beneficial to comprehensively understand the migration of TCS in activated sludge system.

1. Introduction

Triclosan (TCS) is a broad-spectrum antibacterial agent applied in pharmaceutics and personal care products such as soaps, toothpastes, lotions and shampoo (Van Wijnen et al., 2018). With ubiquitous use triclosan is widely found in the environments. Triclosan and its methylated form tend to bioaccumulate, that have been detected in water organisms and even in human milk (Bever et al., 2018; Huo et al., 2018). High environmental risks arise due to the presence of TCS residues, as it has been demonstrated that TCS could be degraded into the toxic dioxin in aquatic systems (Dou et al., 2018; Zhu et al., 2018).

TCS is discharged into the sewage and consequently enters wastewater treatment plants (WWTP). As a hydrophobic organic pollutant with high octanol/water partition coefficient, about 90% TCS can be removed in WWTP employing conventional activated sludge process, of which 30–40% is due to biodegradation while the remainder is adsorbed by the sludge (Chen et al., 2011). Typical concentrations of triclosan in sludge are at 0.028–37.189 mg/kg level (Orhon et al., 2018), revealing that activated sludge has the ability of reserving these compounds through adsorption.

For the previous studies on TCS adsorption, the activated sludge is considered as a whole unit. Actually, as a complex system, the contribution of the sub-fractions of activated sludge to TCS removal are different. Extracellular polymeric substances (EPS), mixture of biomacromolecular polymers secreted by microorganisms, are considered as the major component of activated sludge (Sheng et al., 2010). Various organic contaminants such as phenanthrene, benzene and dyes can be adsorbed by EPS through complicated interactions (Pan et al., 2010a; Sheng et al., 2008; Zhang et al., 2009). Our previous work demonstrates that EPS of activated sludge could bind with sulfonamides through hydrophobic interaction, influencing the distribution of contaminants in activated sludge system (Xu et al., 2013). Winkler et al.

* Corresponding author. Shanghai Key Lab for Urban Ecological Processes and Eco-Restoration, School of Ecological and Environmental Sciences, East China Normal University, Shanghai, China.
** Corresponding author.
E-mail addresses: jxu@des.ecnu.edu.cn (J. Xu), gpsheng@ustc.edu.cn (G.-p. Sheng).

https://doi.org/10.1016/j.jenvman.2018.11.059
Received 6 September 2018; Received in revised form 19 October 2018; Accepted 15 November 2018
Available online 23 November 2018
0301-4797/

reported that TCS bound to the EPS of sludge in the oxidation ditch interfered the effluent quality, as the bound TCS might be released from EPS in the final clarifier (Winkler et al., 2007). Thus, the binding interactions between EPS and TCS directly influence the removal of TCS. However, the binding properties of sludge EPS to TCS have never been addressed until now.

The binding process between EPS and contaminants could be influenced by many factors, leading to variation of adsorption ability of activated sludge. It was found that the adsorption of activated sludge to humus enhanced with the decreased pH value, attributing to the hydrophobic interaction between humic acid and EPS. With the addition of Ca^{2+}, the adsorption rate can be improved by Ca^{2+} bridging between EPS and humus (Sheng et al., 2010). In addition, different subfraction of EPS including loosely bound EPS (LB-EPS) and tightly bound EPS (TB-EPS) might have different contributions to the binding process. LB-EPS is a loose and dispersible slime layer without obvious edge, while TB-EPS form a certain shape, tightly binding with the microbial cells (Sheng et al., 2010). Compared with TB-EPS, the contaminants bound to LB-EPS might be more easily released with the solubilization of LB-EPS into the surrounding environment (Pan et al., 2010b). Therefore, it is necessary to understand the differences between LB-EPS and TB-EPS in their binding properties to the contaminants.

In this work, the binding properties of LB-EPS and TB-EPS of activated sludge to TCS are investigated by fluorescence quenching approach. The influences of aquatic conditions including solution pH, ionic strength and temperature on the interactions between EPS and TCS are explored. Possible interaction mechanisms are discussed as well as the corresponding environmental implication. This work would highlight the important roles of EPS in TCS removal, that is beneficial to comprehensively understand the migration of TCS in activated sludge system.

2. Materials and methods

2.1. EPS extraction and analysis

Activated sludge was collected from the aeration tank of Wangtang municipal wastewater treatment plant, Hefei, China. LB-EPS and TB-EPS were extracted by modified heat extraction method (Xu et al., 2016). 50 mL sludge suspension was centrifugated at 4000 g for 5 min. The settled sludge was resuspended to 50 mL by 0.1 M NaCl preheated to 60 °C. The sludge suspension was shake for 1 min by vortex mixer (Maxi Mix II, Thermolyne), and then centrifuged at 4000 g for 10 min. The supernatant was considered as LB-EPS. Afterwards, the sludge pellet was resuspended in 0.1 M NaCl of 50 mL. The sludge suspension was heated to 60 °C by water bath for 30 min, followed by centrifugation at 4000 *g* for 15 min. The supernatant collected was considered as TB-EPS. EPS for TCS release experiment were prepared by directly heating the sludge suspension to 60 °C in a water bath for 30 min, which comprised both LB- and TB-EPS.

All the sub-fractions of EPS were filtrated through 0.45-μm membrane for components analysis. Measurement methods for carbohydrates, proteins and humic acids in EPS were described in our previous work (Xu et al., 2013). The concentration of EPS was quantified by the total organic carbon (TOC, TOC-Vcpnanalyzer, Shimadzu).

2.2. EPS and TCS binding experiments

Firstly, series of glass tubes were filled with 5 mL EPS solution respectively. Then TCS of gradient amounts were dosed into the tubes, and 0.1 M NaCl were replenished to keep the final volume to 10 mL. The concentrations of TCS in the glass tubes were controlled at 0–5 mg/L. The solution pH was adjusted with 0.1 M NaOH and 0.1 M HCl, while the ionic strength was adjusted with 2.5 M NaCl. Afterwards, the solution was mixed by oscillator for fluorescence analysis within 4 h after equilibrium. The experiments were conducted at the designed temperature of 4, 25 and 35 °C.

2.3. Free TCS release experiments

250 mg/L EPS solution of different pHs and ionic strengths were prepared. Then TCS was added into the EPS solution to a final concentration of 1 mg/L. After interacting for 1 h, 10 mL EPS-TCS mixture was transferred into a ultrafiltration centrifuge tube (Amicon Ultra-15 30K, Millipore, USA). The solution was centrifuged at 2000 g for 3 min, and free EPS and water passed through the ultrafiltration membrane module in the centrifuge tube to form a filtrate of 0.75 mL. The TCS concentration in the filtrate was determined by HPLC (HPLC-1100, Agilent, USA), which was considered as the concentration of free TCS in EPS-TCS mixture. Thus, the free TCS ratio was calculated as the ratio of free TCS concentration to original TCS concentration (1 mg/L).

2.4. Three-dimensional excitation-emission matrix (EEM) fluorescence spectroscopy

EEM spectra were collected on a luminescence spectrometer (LS-55, Perkin-Elmer Co.,USA). The emission wavelength was set from 300 to 550 nm at 0.5 nm increments, while excitation wavelength ranged from 200 to 400 nm at 10 nm increments. Second order Raleigh light scattering was eliminated by applying a 290 nm emission cutoff filter. Excitation and emission slits were 10 nm with scanning speed of 1200 nm/min. The distilled water was recorded as the background. Matlab 2015b (MathWorks Inc.,USA) was used for dealing with the EEM data.

Parallel factor analysis (PARAFAC) was used to resolve the EEM data. Firstly, the raw EEM data were corrected with the background. Then, the EEM data close to the Rayleigh scattering line were set as zero to eliminate the interfere of the Rayleigh scattering. Afterwards, the three-way data array of EEM was decomposed into a number of trilinear components by PARAFAC analysis. The fluorescence intensity score corresponding to EPS components in each EEM could be obtained. The detailed information about the PARAFAC was described in the previous study (Li et al., 2008).

2.5. Other analysis

The UV-VIS spectra of LB- and TB-EPS were collected on the spectrophotometer (UV-4500, Shimadzu Co.,Japan) at different TCS dosages from 1 to 5 mg/L. The wavelength ranged from 250 to 325 nm. Zeta potential of LB- and TB-EPS at different pH values were determined by zeta potential analyzer (NANO ZS3600, Malvern Co.,UK) at 25 °C. The functional groups of EPS were characterized by FTIR (Nicolet iS50, Thermo Co.,USA). The EPS samples were lyophilized (ZX-27 Freeze Dryer, ZhiXinCo.,China) and mixed with KBr powder, compressing into tables before measurements.

Table 1
EPS components analysis.

Sample	Polysaccharides (mg/L)	Proteins (mg/L)	Humic acids (mg/L)	TOC (mg C/L)
LB-EPS	4.19 ± 0.28	22.58 ± 1.68	17.77 ± 1.14	60.61 ± 3.57
TB-EPS	41.12 ± 3.69	255.20 ± 7.33	319.88 ± 6.89	556.84 ± 9.24

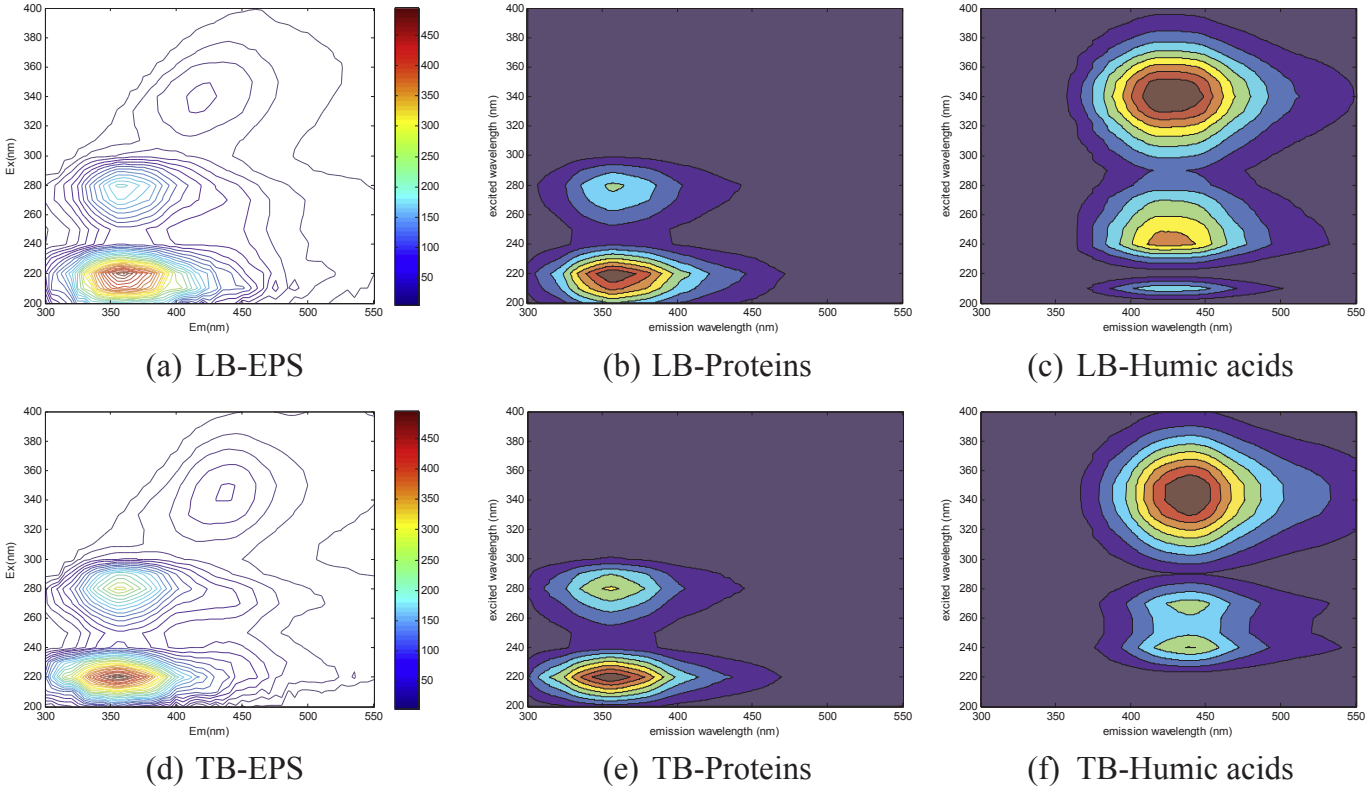

Fig. 1. EEM fluorescence spectra of: (a) (d) EPS; and the two main components in EPS: (b) (e) proteins and (c) (f) humic acids.

3. Results and discussion

3.1. Properties of EPS

The chemical components of LB and TB-EPS were listed in Table 1. Compared to LB-EPS, the concentrations of polysaccharides, proteins, humic acids as well as TOC were much higher for TB-EPS. The proteins and humic acids exhibited obvious quantity advantages over the polysaccharides both in LB and TB-EPS. What's more, the ratio of proteins to humic acids for LB-EPS was higher than TB-EPS.

Fig. 1a, d showed the EEM spectra of LB- and TB-EPS, respectively. Based on PARAFAC analysis, two main components of EPS were identified, excitation/emission 220/345–350 nm (Peak T) shown in Fig. 1b, e and 240–250/450 nm (Peak C) shown in Fig. 1c, f. Peak T belonged to the proteins of EPS, which was caused by the tryptophan residues in the proteins (Baker, 2001). Peak C was attributed to the humic acids of EPS (Baker, 2001). There was no significant difference in main components of LB- and TB-EPS except that the emission wavelength of Peak T for TB-EPS had a slight redshift.

The FTIR spectra in Fig. 2 flected the functional groups of EPS, that were closely related to the specific chemical properties. The peak at 3413 cm^{-1} was attributed to O—H stretching (Braissant et al., 2007). The peak at 2925 cm^{-1} corresponded to C—H stretching. The peak at 1641 cm^{-1} was mainly assigned to C═O and C═C stretching in proteins (Yuan et al., 2011). Near 1400 cm^{-1}, it was considered to be the symmetric stretching vibration of C═O from carboxylic groups (Ueshima et al., 2008). The band near 1240 cm^{-1} was associated with the N—H bending (Coates, 2006). The minor peak around 980 cm^{-1} was thought to be vibration of C═OH, C═O═C and C═C or asymmetric stretching vibration of P═O from polysaccharides and phosphodiesters (Gao and Chorover, 2009). The peaks of 2925 $cm^{-1}$for C—H stretching and 1240 cm^{-1} for N—H bending only presented in LB-EPS not TB-EPS, implying that LB-EPS might contain more amino groups than TB-EPS. The results agreed with the higher ratio of proteins in LB-EPS based on chemical analysis. That would cause the discrepancy between LB- and TB-EPS when they interacted with TCS.

Zeta potential of LB- and TB-EPS under acidic (pH = 3), neutral (pH = 7) and alkaline (pH = 11) conditions were shown in Fig. 2b. Results indicated that both LB- and TB-EPS were negatively charged. With the increasing pH, more negative charges were carried by the EPS samples. Whereas, the absolute value of zeta potential for TB-EPS was larger than LB-EPS under the experimental conditions, meaning that TB-EPS exhibited stronger electronegativity in solution compared to LB-EPS. This was probably due to more amino groups of positively charged existed in LB-EPS as indicated in FTIR analysis. What's more, zeta potential of LB-EPS is approaching the isoelectric point when the pH decreased to 3.

3.2. Mechanisms of the interactions between EPS and TCS

EEM Fluorescence quenching method was applied to investigate the binding interactions between EPS and TCS. Generally, there were two types of quenching process including static quenching (formation of non-fluorescent complex between fluorophore and quencher) and dynamic quenching (quenching caused by collision between fluorophore and quencher).

Stern-Volmer equation was used to verify the mechanism of EPS fluorescence quenching by TCS as follows (Xu et al., 2013):

$$\frac{F_0}{F} = 1 + K_q \tau_0 [Q]_{TCS} \quad (1)$$

where $F_0$was fluorescence intensity score of EPS in the absence of TCS by PARAFAC analysis, F was EPS fluorescence intensity score with addition of TCS, $[Q]_{TCS}$was the concentration of TCS added, $\tau_0$was the average lifetime of EPS (10^{-8} s) (Hu et al., 2009). If quenching constant K_q was larger than 2.0×10^{10} L/mol/s, static quenching dominated the quenching process (Xu et al., 2013). As shown in Table 2, the K_q values obtained were far above 2.0×10^{10} L/mol/s, revealing static quenching due to the formation of EPS-TCS complex (Xu et al., 2013).

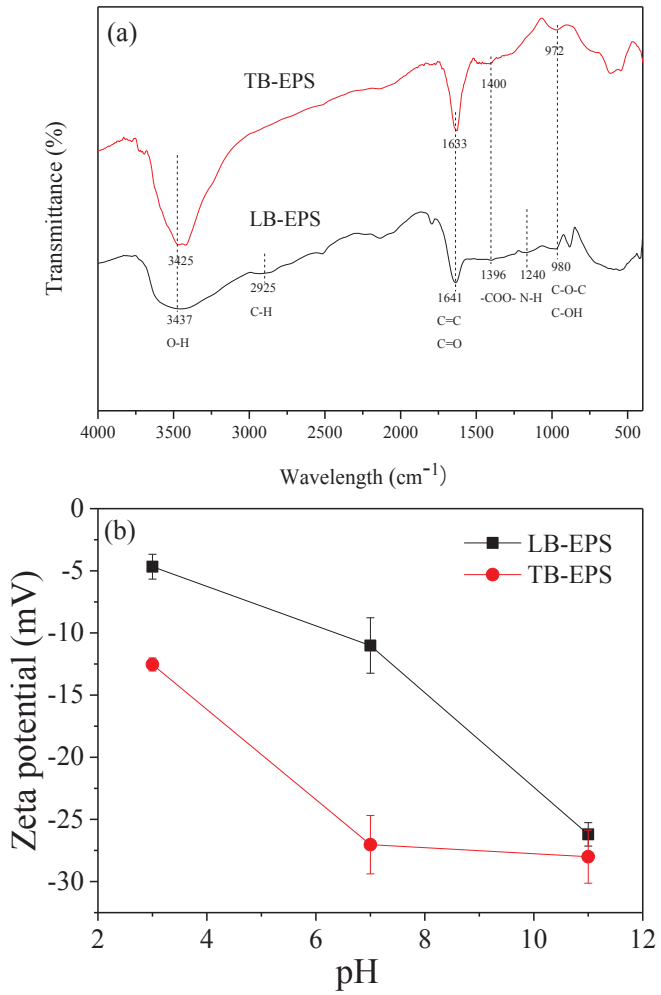

Fig. 2. Characterization of EPS: (a) FTIR spectra (b) Zeta potential values.

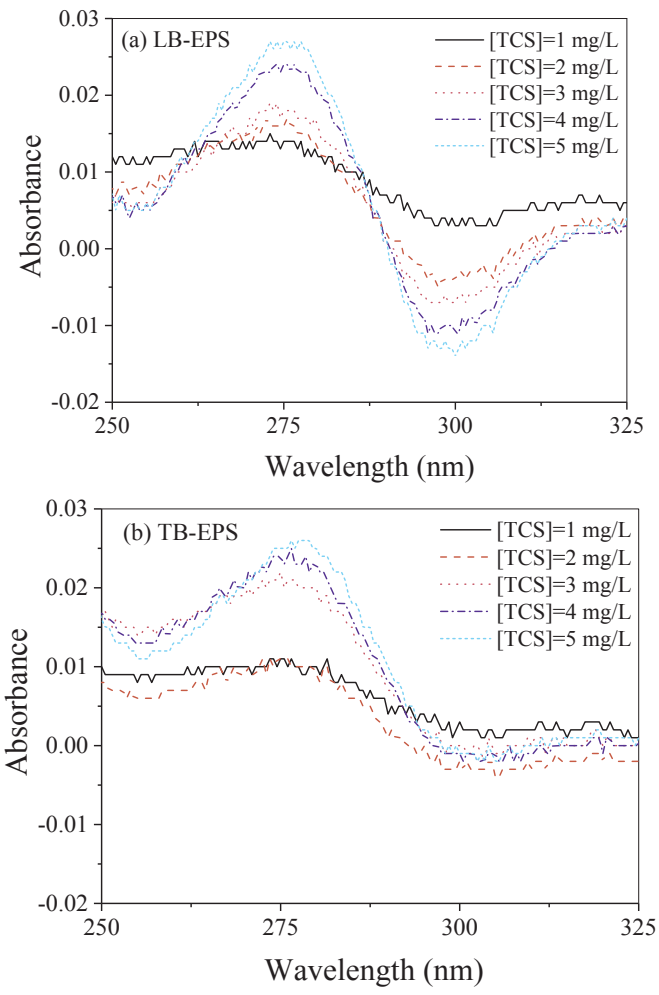

Fig. 3. Differentiated spectra between EPS, TCS and the EPS-TCS complex at various TCS dosages (a) LB-EPS (b) TB-EPS.

UV–Visible absorbance spectra of EPS, TCS and EPS-TCS complex could further illustrate the reason for fluorescence quenching of EPS by TCS. The absorbance spectra of EPS and TCS mixture solution would be the sum of EPS and TCS spectra if the quenching was induced by molecular collision (Xu et al., 2013). However, the differentiated spectrum shown in Fig. 3 indicated that the absorbance spectra of EPS-TCS complex were distinct with the mixture of EPS and TCS spectra. The formation of EPS-TCS complex led to a significant variation in the absorbance spectra. The peak at 280 nm presented in both Fig. 3a and b belonged to TCS, due to the different concentrations of free TCS in solution after binding with EPS. A new peak appeared at 300 nm when TCS bound to LB-EPS while no new peak was observed for TB-EPS. The results implied that the complex formed between TCS and EPS was different for LB- and TB-EPS.

For a binding process involving static quenching mechanism, the apparent binding constant (logK) and the number of binding sites (n) could be determined using the modified double logarithmic equation (Veeralakshmi et al., 2017). This model was based on the assumption that TCS binding independently to a set of equivalent sites on the EPS:

$$\log\frac{F_0 - F}{F} = \log K + n\log[Q]_{TCS} \quad (2)$$

The binding constants and the number of binding sites at 4, 25 and 35 °C were calculated in Table 2. The binding of TCS to proteins was significant while binding of TCS to humic acids could be only observed under 4 °C. Results indicated that the proteins components of EPS dominated the binding process. The binding constants of proteins

Table 2
The quenching constants (Kq), binding constants (logK) and binding sites (n) of the interactions between EPS and TCS at various temperature (pH 7, ionic strength 100 mM).

T (°C)	Proteins						Humic acids					
	LB-EPS			TB-EPS			LB-EPS			TB-EPS		
	Kq ($\times 10^{12}$)	logK	n	Kq ($\times 10^{12}$)	logK	n	Kq ($\times 10^{12}$)	logK	n	Kq ($\times 10^{12}$)	logK	n
4	1.33	4.84	1.16	0.95	4.48	1.10	0.87	3.12	0.82	0.97	3.38	0.87
25	1.89	4.50	1.01	1.55	4.18	0.94	a	a	a	a	a	a
35	2.27	4.39	1.01	2.57	4.01	0.91	a	a	a	a	a	a

a No significant fluorescence quenching was observed.

Table 3
Thermodynamic parameters of the interactions between EPS and TCS.

T (°C)	LB-EPS				TB-EPS			
	ΔG (KJ/mol)	ΔH (KJ/mol)	ΔS (J/mol/K)	R^2	ΔG (KJ/mol)	ΔH (KJ/mol)	ΔS (J/mol/K)	R^2
4	−11.131	−10.436	2.51	0.99	−10.306	−9.639	2.42	0.99
25	−11.183				−10.360			
35	−11.209				−10.384			

decreased with the increasing temperature, suggesting the exothermic properties of the interactions. The decreasing binding sites with raising temperature was related to configuration changes of the proteins. The binding constants of LB-EPS were higher than TB-EPS under all temperatures, implying that LB-EPS had stronger affinity to TCS than TB-EPS.

Possible mechanisms of interactions between TCS and EPS could be deduced from the thermodynamic parameters of the interactions. As summarized in Table 3, Gibbs free energy change (ΔG), enthalpy change (ΔH) and entropy change (ΔS) of the interactions were calculated. ΔH and ΔS were fitted by Van't Hoff Equation (Ross and Subramanian, 1981), which assumed that ΔH and ΔS were constants since the temperature did not change in large scale (Zhang et al., 2008).

$$\log K = -\frac{\Delta H}{RT} + \frac{\Delta S}{R} \quad (3)$$

where R was the universal gas constant, 8.314 J/mol/K, T was the absolute temperature (K), logK represented the binding constants obtained by double logarithm regression. Then, ΔG could be calculated as follows (Ross and Subramanian, 1981):

$$\Delta G = \Delta H - T\Delta S \quad (4)$$

As shown in Table 3, the negative ΔG values indicated that both LB and TB-EPS could bind with TCS spontaneously. The negative ΔH values suggested that the binding process of TCS to EPS was exothermic. The positive ΔS values revealed that the disorder degree of the system increased with the formation of EPS-TCS complex. The thermodynamic parameters also implied the driven force of the interactions between EPS and TCS. The negative ΔH value suggested the existence of hydrogen bond and electrostatic effect (Veeralakshmi et al., 2017). Hydrogen bond could be formed between phenolic hydroxyl in TCS and carbonyl oxygen in proteins (Chen et al., 2012). Although the negative ΔH was also taken as the evidence of electrostatic effect, the prevalence of TCS of molecular form at pH 7 made it less significant (Fig. 4). The positive ΔS value was frequently considered as hydrophobic interaction

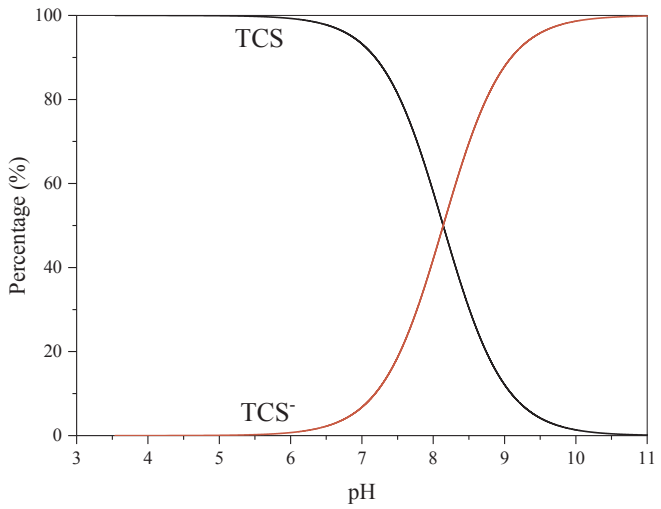

Fig. 4. Proportion of TCS and anionic TCS (TCS^-) in dependent on solution pH.

(Ross and Subramanian, 1981). It was reported that aromatic ring in TCS could interact with amino acid residues in proteins by hydrophobic interaction (Chen et al., 2012). Hydrogen bonds could reduce the disorder degree of the system, offsetting part of the positive ΔS generated by hydrophobic interaction (Veeralakshmi et al., 2017). Considering $|\Delta H| > |T\Delta S|$, the binding reaction was mainly driven by hydrogen bonds and hydrophobic interaction under the experimental condition (pH 7, ionic strength 100 mM). However, with the variation of solution pH and ionic strength, electrostatic interactions would play crucial roles in the binding process since the charges of both EPS and TCS were altered with aquatic conditions.

3.3. Interactions between TCS and EPS at various pH values

The interactions between TCS and EPS were investigated at various pH values, with corresponding binding constants and binding sites calculated in Table 4. The binding constants for the proteins were several orders of magnitude higher than those of humic acids, no matter LB-EPS and TB-EPS. The results indicated TCS was mainly bound to the proteins components in EPS.

Solution pH had obvious influences on the interactions between EPS and TCS. For LB-EPS, the binding constant increased with the raising pH ranged from 3 to 9, then slightly decreased at pH 11. The evolution profile of the binding sites was similar to that of the binding constants. This was probably attributed to the configuration changes of LB-EPS depending on solution pH. It was found that zeta potential of LB-EPS was −4.26& mV at pH 3 (Fig. 2b), almost reaching the isoelectric point. EPS tended to form aggregates around isoelectric point whose geometrical specific surface area comparatively decreased to some extent (Wang et al., 2012). Consequently, the active sites exposed for binding with TCS were reduced with aggregation, leading to the lower binding constants and binding sites. With the increasing pH, the molecular chains of LB-EPS would extend, forming lower density structure and exposing more geometrical surface area, that was beneficial to bind with TCS (Wang et al., 2012). However, with further increasing pH to 11, TCS of anionic form predominated (Fig. 4) as TCS mainly existed in deprotonated form when pH was higher than 8.14. As the electronegativity of LB-EPS colloids also increased with the elevating pH, electrostatic repulsion between LB-EPS and TCS would weaken the binding strength. The highest binding constant was observed at pH 9, that might be mainly due to the extended configuration of LB-EPS,

Table 4
The binding constants (logK) and binding sites (n) of the interactions between EPS and TCS at various pH values (ionic strength 100 mM, 25 °C).

pH	Proteins				Humic acids			
	LB-EPS		TB-EPS		LB-EPS		TB-EPS	
	logK	n	logK	n	logK	n	logK	n
3	3.92	0.93	5.05	1.16	2.21	0.70	1.74	0.60
5	4.18	0.99	4.30	0.94	2.48	0.78	a	a
7	4.50	1.01	4.18	0.94	a	a	a	a
9	6.15	1.32	6.19	1.43	a	a	a	a
11	5.34	1.21	5.68	1.30	a	a	a	a

a No significant fluorescence quenching was observed.

Table 5
The binding constants (logK) and binding sites (n) of the interactions between EPS and TCS at various ionic strengths (pH 7, 25 °C).

Ionic strength (mM)	Proteins				Humic acids			
	LB-EPS		TB-EPS		LB-EPS		TB-EPS	
	logK	n	logK	n	logK	n	logK	n
100	4.50	1.01	4.18	0.94	a	a	a	a
200	3.69	0.82	3.91	0.97	2.75	0.81	2.29	0.65
500	5.04	1.11	4.18	0.94	4.21	1.05	4.12	1.01
1000	3.90	0.83	4.10	0.94	3.64	1.02	3.94	0.97

a No significant fluorescence quenching was observed.

facilitating the binding process of EPS and TCS in spite of the existence of electrostatic repulsion.

TB-EPS showed similar complexing abilities with LB-EPS at various pH values except that the binding strength was relatively strong at pH 3. This result implied that the interaction mechanism of TB-EPS and TCS might have changed under the condition of pH 3. It was reported that acidic condition favored hydrophobic interactions between the organic matter and the target molecules as they were both in molecular form (Tohidi and Cai, 2016). Thus, hydrophobic forces rather than hydrogen bond and electrostatic effect dominated the interactions between TB-EPS and TCS at pH 3.

3.4. Interactions between TCS and EPS at various ionic strengths

The binding constants and binding sites of TCS and EPS at various ionic strengths were listed in Table 5. The binding strength of LB- and TB-EPS to TCS showed similar evolution trend with increasing ionic strength under pH 7. Ionic strength could influence the binding process of EPS and TCS by affecting hydrogen bond, electrostatic effect and hydrophobic force simultaneously. When the ionic strength was 500 mM, the highest binding constants were achieved for both proteins and humic acids.

Ionic strength could play positive roles in the binding process of EPS and TCS. On one hand, thickness of EPS electric double-layers was compressed by increasing the ionic strength, weakening the electrostatic repulsion between EPS and TCS (Tsapikouni and Missirlis, 2007). On the other hand, high ionic strength decreased the hydration of TCS and EPS, promoting the formation of hydrogen bonds between them (Wang et al., 2015). However, too high ionic strength inhibited the binding process, since the binding constants decreased obviously for both proteins and humic acids when the ionic strength was 1000 mM. This was due to the aggregation of EPS induced by salting out effect. That would reduce the specific surface and binding sites of EPS participated in the binding process (Tsapikouni and Missirlis, 2007). It was noticed that the binding constants of proteins declined when ionic strength raise from 100 mM to 200 mM. This might be related to the increased solubility of TCS, since it was reported that the solubility of TCS would increase with ionic strength in the presence of polysaccharides with carboxyl (Wu et al., 2015). TCS tended to partition in water phase rather than complexing with EPS, leading to the decreased binding constant. Overall, influences of ionic strength on the binding process of EPS and TCS were complicated depending on concentration range.

4. Environmental implication

TCS could interact with LB- and TB-EPS to form relative stable complex spontaneously. Generally, LB-EPS have a stronger binding ability to TCS than TB-EPS under neutral environment. The stability of TCS-EPS complex are mainly sustained by hydrogen bonds, electrostatic effect and hydrophobic interactions, which could be interfered by

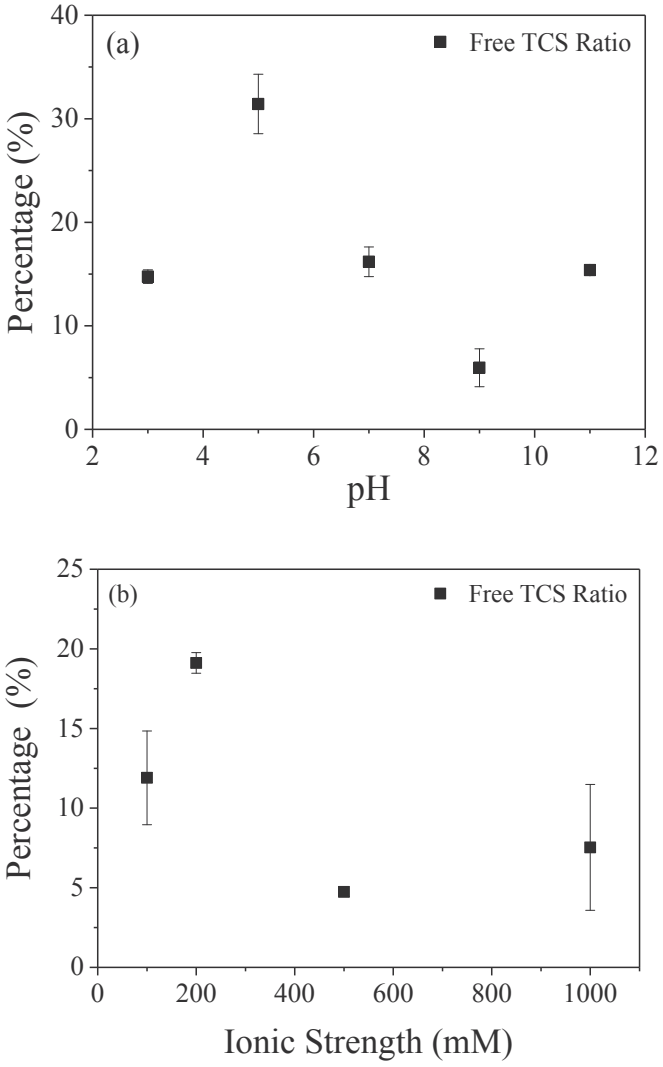

Fig. 5. Proportion of free TCS under different pH values (a) and ionic strength (b).

environmental conditions. As EPS cover the outside surface of activated sludge, the contaminants bound to EPS might be more easily released into the surrounding environment. For example, if the temperature increased, TCS would be probably disassociated from EPS of activated sludge into water as the binding strength is weakened. This can explain the sudden increase of TCS concentration in the effluent, which originates from the EPS-TCS complex responding to environmental changes. To provide the evidences of TCS release from EPS under different environmental conditions, the experiments of free TCS released from EPS were conducted and results were shown in Fig. 5. It was clear that the ratio of free TCS varied with different environmental conditions. When pH was 5, the free TCS ratio was at a high level of 30% (Fig. 5a), which were generally identical with the low value of binding constant at pH 5 (Table 4). Similarly, When ionic strength was 200 mM, the free TCS ratio was about 20% (Fig. 5b), corresponding to the weak binding affinity of TCS to EPS under this ionic strength (Table 4). Results proved that the proportion of free TCS was altering in the EPS-TCS mixture with aquatic conditions. TCS would be disassociated from EPS into water when the binding strength was reduced under the unfavorable condition.

Also, this work brings some insights into wastewater treatment process, since the operation parameters have significant influences on the properties of sludge EPS including their amounts, composition and proportions of LB- and TB-EPS. Sludge retention time (SRT) is one of the

most important parameters affecting sludge EPS, as EPS are mainly produced during the exponential growth phase and then consumed (Sheng et al., 2006). It was found that LB-EPS, which played crucial roles in the binding process with TCS, decreased dramatically with increasing SRT while TB-EPS showed no distinct relationship with SRT (Li and Yang, 2007). Thus, appropriate regulation to avoid too long SRT is essential to maintain a satisfactory performance in TCS removal during wastewater treatment. In addition, wastewater of high nutrient levels would improve EPS production, especially when P is in short supply while C and N are sufficient (Sheng et al., 2010). Thus, under the condition of high nutrient concentrations in wastewater, organic micropollutant such as TCS are more likely to be retained in sludge EPS rather than releasing into the water environment. The ratio of C/N in wastewater is also an important factor influencing the composition of EPS. It was demonstrated that proportion of proteins in EPS decreased rapidly with the increasing C/N ratio (Durmaz and Sanin, 2001). As TCS are mainly bound with proteins component in EPS, considerable risk of TCS release would be generated for high C/N ratio of wastewater. Generally, the operation parameters and influent quality greatly influence the properties of sludge EPS, consequently affecting their binding affinity to TCS. To obtain a good wastewater treatment performance, not only COD, N and P removal but also the re-release of micropollutants such as TCS from sludge EPS need to be considered during the process of adjusting operation parameters.

5. Conclusions

This work investigated the interactions between LB- and TB-EPS of activated sludge and TCS under different aquatic conditions. Results indicated that binding processes of EPS to TCS were exothermic mainly driven by the enthalpy changes. The proteins components in EPS dominated the binding process by hydrogen bonds and hydrophobic interaction. The binding strength could be improved under the condition of weak alkaline and relative high ionic strength. Generally, LB-EPS exhibited stronger binding ability to TCS than TB-EPS under neutral environment, playing more crucial roles in the binding process. This work identified the important contributions of EPS to TCS removal, that was beneficial to better understand the migration of TCS in activated sludge system.

Acknowledgements

The authors wish to thank National Natural Science Foundation of China (51708224) for the support of this study.

References

Baker, A., 2001. Fluorescence excitation-emission matrix characterization of some sewage-impacted rivers. Environ. Sci. Technol. 35, 948–953.
Bever, C.S., Rand, A.A., Nording, M., Taft, D., Kalanetra, K.M., Mills, D.A., Breck, M.A., Smilowitz, J.T., German, J.B., Hammock, B.D., 2018. Effects of triclosan in breast milk on the infant fecal microbiome. Chemosphere 203, 467–473.
Braissant, O., Decho, A.W., Dupraz, C., Glunk, C., Przekop, K.M., Visscher, P.T., 2007. Exopolymeric substances of sulfate-reducing bacteria: interactions with calcium at alkaline pH and implication for formation of carbonate minerals. Geobiology 5, 401–411.
Chen, J., Zhou, X., Zhang, Y., Zi, Y., Qian, Y., Gao, H., Lin, S., 2012. Binding of triclosan to human serum albumin: insight into the molecular toxicity of emerging contaminant. Environ. Sci. Pollut. Res. 19, 2528–2536.
Chen, X.J., Nielsen, J.L., Furgal, K., Liu, Y.L., Lolas, I.B., Bester, K., 2011. Biodegradation of triclosan and formation of methyl-triclosan in activated sludge under aerobic conditions. Chemosphere 84, 452–456.
Coates, J., 2006. Interpretation of Infrared Spectra, aPractical Approach. John Wiley & Sons, Ltd.
Dou, R.N., Wang, J.H., Chen, Y.C., Hu, Y.Y., 2018. The transformation of triclosan by laccase: effect of humic acid on the reaction kinetics, products and pathway. Environ. Pollut. 234, 88–95.
Durmaz, B., Sanin, F.D., 2001. Effect of carbon to nitrogen ratio on the composition of microbial extracellular polymers in activated sludge. Water Sci. Technol. 221–229.
Gao, X., Chorover, J., 2009. In-situ monitoring of Cryptosporidium parvum oocyst surface adhesion using ATR-FTIR spectroscopy. Colloids Surf., B 71, 169–176.
Hu, Y.J., Liu, Y., Xiao, X.H., 2009. Investigation of the interaction between Berberine and human serum albumin. Biomacromolecules 10, 517–521.
Huo, W.Q., Xia, W., Wu, C.S., Zhu, Y.S., Zhang, B., Wan, Y.J., Zhou, A.F., Qian, Z.M., Chen, Z., Jiang, Y.Q., Liu, H.X., Hu, J., Xu, B., Xu, S.Q., Li, Y.Y., 2018. Urinary level of triclosan in a population of Chinese pregnant women and its association with birth outcomes. Environ. Pollut. 233, 872–879.
Li, W.H., Sheng, G.P., Liu, X.W., Yu, H.Q., 2008. Characterizing the extracellular and intracellular fluorescent products of activated sludge in a sequencing batch reactor. Water Res. 42, 3173–3181.
Li, X.Y., Yang, S.F., 2007. Influence of loosely bound extracellular polymeric substances (EPS) on the flocculation, sedimentation and dewaterability of activated sludge. Water Res. 41, 1022–1030.
Orhon, A.K., Orhon, K.B., Yetis, U., Dilek, F.B., 2018. Fate of triclosan in laboratory-scale activated sludge reactors - effect of culture acclimation. J. Environ. Manag. 216, 320–327.
Pan, X.L., Liu, J., Zhang, D.Y., 2010a. Binding of phenanthrene to extracellular polymeric substances (EPS) from aerobic activated sludge: afluorescence study. Colloids Surf., B 80, 103–106.
Pan, X.L., Liu, J., Zhang, D.Y., Chen, X., Song, W.J., Wu, F.C., 2010b. Binding of dicamba to soluble and bound extracellular polymeric substances (EPS) from aerobic activated sludge: afluorescence quenching study. J. Colloid Interface Sci. 345, 442–447.
Ross, P.D., Subramanian, S., 1981. Thermodynamics of protein association reactions: forces contributing to stability. Biochemistry 20, 3096–3102.
Sheng, G.P., Yu, H.Q., Li, X.Y., 2010. Extracellular polymeric substances (EPS) of microbial aggregates in biological wastewater treatment systems: areview. Biotechnol. Adv. 28, 882–894.
Sheng, G.P., Yu, H.Q., Li, X.Y., 2006. Stability of sludge flocs under shear conditions: roles of extracellular polymeric substances (EPS). Biotechnol. Bioeng. 93, 1095–1102.
Sheng, G.P., Zhang, M.L., Yu, H.Q., 2008. Characterization of adsorption properties of extracellular polymeric substances (EPS) extracted from sludge. Colloids Surf., B 62, 83–90.
Tohidi, F., Cai, Z., 2016. Adsorption isotherms and kinetics for the removal of triclosan and methyl triclosan from wastewater using inactivated dried sludge. Process Biochem. 51, 1069–1077.
Tsapikouni, T.S., Missirlis, Y.F., 2007. pH and ionic strength effect on single fibrinogen molecule adsorption on mica studied with AFM. Colloids Surf., B 57, 89–96.
Ueshima, M., Ginn, B.R., Haack, E.A., Szymailowski, J.E.S., Fein, F.B., 2008. Cd adsorption onto Pseudomonas putida in the presence and absence of extracellular polymeric substances. Geochem. Cosmochim. Acta 72, 5885–5895.
Van Wijnen, J., Ragas, A.M.J., Kroeze, C., 2018. River export of triclosan from land to sea: aglobal modelling approach. Sci. Total Environ. 621, 1280–1288.
Veeralakshmi, S., Sabapathi, G., Nehru, S., Venuvanalingam, P., Arunachalam, S., 2017. Surfactant–cobalt(III) complexes: the impact of hydrophobicity on interaction with HSA and DNA –insights from experimental and theoretical approach. Colloids Surf., B 153, 85–94.
Wang, L.L., Wang, L.F., Ren, X.M., Ye, X.D., Li, W.W., Yuan, S.J., Sun, M., Sheng, G.P., Yu, H.Q., Wang, X.-K., 2012. pH dependence of structure and surface properties of microbial EPS. Environ. Sci. Technol. 46, 737–744.
Wang, L., Cao, Y., Zhang, K., Fang, Y., Nishinari, K., Phillips, G.O., 2015. Hydrogen bonding enhances the electrostatic complex coacervation between κ-carrageenan and gelatin. Colloid. Surface.A 482, 604–610.
Winkler, G., Fischer, R., Krebs, P., Thompson, A., Cartmell, E., 2007. Mass flow balances of triclosan in rural wastewater treatment plants and the impact of biomass parameters on the removal. Eng. Life Sci. 7, 42–51.
Wu, W., Hu, Y., Guo, Q., Yan, J., Chen, Y., Cheng, J., 2015. Sorption/desorption behavior of triclosan in sediment–water–rhamnolipid systems: effects of pH, ionic strength, and DOM. J. Hazard Mater. 297, 59–65.
Xu, J., Sheng, G.P., Ma, Y., Wang, L.F., Yu, H.Q., 2013. Roles of extracellular polymeric substances (EPS) in the migration and removal of sulfamethazine in activated sludge system. Water Res. 47, 5298–5306.
Xu, J., Yu, H.Q., Li, X.Y., 2016. Probing the contribution of extracellular polymeric substance fractions to activated-sludge bioflocculationusing particle image velocimetry in combination with extended DLVO analysis. Chem. Eng. J. 303, 627–635.
Yuan, S.J., Sun, M., Sheng, G.P., Li, Y., Li, W.W., Yao, R.S., Yu, H.Q., 2011. Identification of key constituents and structure of the extracellular polymeric substances excreted by bacillus megaterium TF10 for their flocculation capacity. Environ. Sci. Technol. 45, 1152–1157.
Zhang, Y.Z., Zhou, B., Liu, Y.X., Zhou, C.X., Ding, X.L., Liu, Y., 2008. Fluorescence study on the interaction of bovine serum albumin with p-aminoazobenzene. J. Fluoresc. 18, 109–118.
Zhang, Z.Q., Xia, S.Q., Wang, X.J., Yang, A., Xu, B., Chen, L., Zhu, Z.L., Zhao, J.F., Jaffrezic-Renault, N., Leonard, D., 2009. A novel biosorbent for dye removal: extracellular polymeric substance (EPS) of Proteus mirabilis TJ-1. J. Hazard Mater. 163, 279–284.
Zhu, L., Shao, Y., Xiao, H., Santiago-Schübel, B., Meyer-Alert, H., Schiwy, S., Yin, D., Hollert, H., Küppers, S., 2018. Electrochemical simulation of triclosan metabolism and toxicological evaluation. Sci. Total Environ. 622–623, 1193–1201.